A&A manuscript no.
(will be inserted by hand later)

Your thesaurus codes are:
08.06.2; 09.13.2; 09.10.1; 09.09.1; 02.19.1; 02.18.7

ASTRONOMY
AND
ASTROPHYSICS
16.9.1996

Thermal H_2O emission from the Herbig-Haro flow HH 54*

R. Liseau[1,2], **C. Ceccarelli**[3,2], **B. Larsson**[1], **B. Nisini**[2], **G.J. White**[4], **P. Ade**[4], **C. Armand**[5], **M. Burgdorf**[5], **E. Caux**[6], **R. Cerulli**[2], **S. Church**[7], **P.E. Clegg**[4], **A. Di Gorgio**[5,2], **I. Furniss**[8], **T. Giannini**[2], **W. Glencross**[8], **C. Gry**[5,9], **K. King**[10], **T. Lim**[5], **D. Lorenzetti**[11], **S. Molinari**[5,2], **D. Naylor**[12], **R. Orfei**[2], **P. Saraceno**[2], **S. Sidher**[5], **H. Smith**[4], **L. Spinoglio**[2], **B. Swinyard**[10], **D. Texier**[5], **E. Tommasi**[2], **N. Trams**[5], and **S. Unger**[10]

1. Stockholm Observatory, S-133 36, Saltsjöbaden, Sweden, e-mail: rene@astro.su.se
2. CNR-Istituto di Fisica dello Spazio Interplanetario, Casella Postale 27, I-00044 Frascati (Rome), Italy
3. Laboratoire d'Astrophysique de l'Observatoire de Grenoble, 414, rue de la Piscine, BP 53, F-38041 Grenoble, France
4. Physics Department, Queen Mary & Westfield College, University of London, Mile End Road, London E1 4NS, UK
5. The Lws Instrument-Dedicated Team, Iso Science Operations Centre, P.O. Box 50727, 28080 Madrid, Spain
6. Centre d'Etude Spatiale des Rayonnements, BP 4346, 31029 Toulouse cedex, France
7. California Institute of Technology, Pasadena, CA 91125, USA
8. Department of Physics and Astronomy, University College London, Gower Street, London, WC1 E 6BT, UK
9. Laboratoire d'Astronomie Spatiale, BP8, 13376 Marseille cedex 12, France
10. Space Science Department, Rutherford Appleton Laboratory, Chilton, Oxon OX11 OQX, UK
11. Osservatorio Astronomico di Roma, I-00044 Monteporzio, Italy
12. Department of Physics, University of Lethbridge, Lethbridge, Alberta T1K 3M4, Canada

Received date; Accepted date

Abstract. The first detection of thermal water emission from a Herbig-Haro object is presented. The observations were performed with the Lws (Long Wavelength Spectrograph) aboard Iso (Infrared Space Observatory). Besides H_2O, rotational lines of CO are present in the spectrum of HH 54. These high-J CO lines are used to derive the physical model parameters of the Fir (far-infrared) molecular line emitting regions. This model fits simultaneously the observed OH and H_2O spectra for an OH abundance $X(\mathrm{OH}) = 10^{-6}$ and a water vapour abundance $X(\mathrm{H_2O}) = 10^{-5}$.

At a distance of 250 pc, the total CO, OH and H_2O rotational line cooling rate is estimated to be $1.3\,10^{-2}\,\mathrm{L}_\odot$, which is comparable to the mechanical luminosity generated by the $10\,\mathrm{km\,s^{-1}}$ shocks, suggesting that practically all of the cooling of the *weak-shock* regions is done by these three molecular species alone.

Key words: Stars: formation - ISM: molecules - ISM: jets and outflows - ISM: individual objects: HH 54 - Physical processes: Shock waves - Physical processes: Radiative transfer

1. Introduction

The Herbig-Haro object HH 54 is associated with the star forming dark cloud Cha II, at a distance $d = 250$ pc, although this is uncertain by as much as $\gtrsim 100$ pc. The object consists of several arcsecond scale bright knots enveloped by diffuse emission ($\sim 40''$; Graham & Hartigan 1988). The overall optical emission line spectrum is indicative of the presence of relatively highly excited gas and can be explained with J-shocks of velocities of at least $60\,\mathrm{km\,s^{-1}}$ (Schwartz & Dopita 1980). Considerably lower velocities, of $\sim 10\,\mathrm{km\,s^{-1}}$, are observed in the CO (1–0) emission from a cold (~ 15 K), extended molecular flow, whose emission peaks $\gtrsim 3'$ away from HH 54 (Knee 1992). Recent Nir (near-infrared) observations by Gredel (1994) testify to the presence of warm, purely collisionally excited, H_2 gas. This rather hot gas [$\sim 2\,000$ K, $N(\mathrm{H_2}) = 3.6\,10^{17}\,\mathrm{cm^{-2}}$] might be expected to emit strongly in relatively highly excited rotational lines of CO and H_2O. Many of these transitions fall within the waveband of the Lws and in this *Letter* we report on the first detection of thermally excited H_2O emission from an HH flow, as well as observations of lines of CO and OH.

2. Observations

Lws-grating scans (43–196.7 μm, $R = 140-330$), were obtained towards HH 54B ($\alpha = 12^{\mathrm{h}}52^{\mathrm{m}}10\overset{\mathrm{s}}{.}6$, $\delta = -76°40'04''$, equinox 1950.0) during Iso-revolution no. 92 on February

* Based on observations with Iso, an Esa project with instruments funded by Esa Member States (especially the PI countries: France, Germany, the Netherlands and the United Kingdom) and with the participation of Isas and Nasa (see: Kessler et al. 1996).

17, 1996. The instrument and its capabilities are described by Clegg et al. (1996) and by Swinyard et al. (1996) respectively. The absolute flux calibration is based on observations of the planet Uranus (Swinyard et al.). Full grating scans were also obtained towards HH 52, HH 53 and the CO outflow, which was mapped (3×3, 100″ grid). These observations are described by Nisini et al. (1996).

3. Results

The FIR spectrum towards HH 54 consists of emission lines and continuous radiation (Fig. 1). The line spectrum of HH 54 is dominated by [O I] 63 μm, as expected for shocked gas. The [O I] 63/145 μm emission is intrinsic to HH 54 and compatible with the predictions of existing J-shock models, whereas the observed spatial distribution and intensity of the [C II] 158 μm line is characteristic of a PDR at the cloud surface (see: Nisini et al.).

In addition, several, weaker lines are present longward of $\sim 100\,\mu$m, coinciding in wavelength with rotational transitions of CO, H_2O and OH. No such emission could be discerned in any of the other spectra of this region. All the line measurements are given by Nisini et al..

The continuum level is consistent with the sum of the zodiacal and galactic backgrounds and the dark cloud emission determined by IRAS. Situated within HH 54 is the IRAS point source 12522–7640, which has significant flux density only at 60 μm (0.59±0.09 Jy). This flux can probably be ascribed entirely to [O I] line emission, for which we find (corresponding to the IRAS band) $S_{60} = 0.50 \pm 0.03$ Jy, i.e. any *stellar* source would be extremely faint at these wavelengths. We conclude, therefore, that the observed diffuse radiation field is weak, a circumstance that largely simplifies the analysis of the molecular line emission in the following sections.

4. Discussion

4.1. The CO spectrum

CO emission lines from HH 54 were traced from the rotational upper level $J = 14$ to $J \lesssim 19$. The observed decrease in CO line flux with J (Fig. 1) implies that the CO emitting gas is not very highly excited and, consequently, that the emission feature at 113.5 μm is unlikely to be attributable to CO (23–22).

The quite limited spatial ($\sim 80''$) and spectral ($\sim 1\,500\,\mathrm{km\,s^{-1}}$) resolution of the observations justified initially only average values of the physical parameters being estimated. The observed CO line *ratios* are reasonably well fit by a model of HH 54, where the average kinetic temperature of the gas is $T_{\rm kin} = (330 \pm 30)$ K and the logarithmic volume density (in cm^{-3}) is $\log n(\mathrm{H_2}) = 5.3 \pm 0.2$ (Fig. 2). The hydrogen column density of the model, $N(\mathrm{H_2}) = 5.0\,10^{20}\mathrm{cm^{-2}}$, is larger by three orders of magnitude than that of the hot H_2 gas. We assume

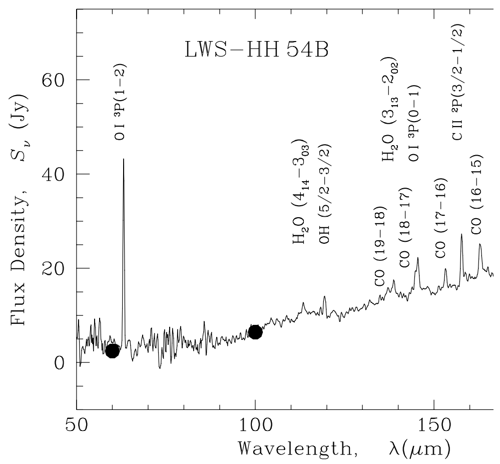

Fig. 1. LWS spectrum towards HH 54 with emission lines identified. The oversampled data have been rebinned and smoothed with a running mean filter to $\Delta\lambda = 0.42\,\mu$m. The filled dots refer to IRAS data (PSC 2 + LRP + *zodiacal background*)

that the relative abundance of carbon monoxide molecules $X(\mathrm{CO}) = [N(\mathrm{CO})/N(\mathrm{H_2})] = 8\,10^{-5}$.

Further, the *absolute* flux level of the observed CO lines then implies that only about $f_{\rm b} = (10 \pm 2)^{-1}$ of the LWS-beam is filled by the emission. Hence, we derive the CO source size $\sim 25''$ to 30″ (0.03 pc), comparable to the extent of HH 54 at optical and NIR wavelengths.

The excitation and radiative transfer calculations were all performed in the Sobolev approximation using a Large Velocity Gradient code. The Einstein A values and energies were adopted from Chackerian & Tipping (1983), with collisional excitation rate coefficients, extrapolated beyond $J = 20$ to $J = 25$, being taken from Schinke et al. (1985). An intrinsic line width of $10\,\mathrm{km\,s^{-1}}$ was adopted, a choice which will be justified below (sect. 4.3), and all CO transitions were found to be optically thin. Our model of the CO emission is not particularly sensitive to the choice of line widths, as long as $\Delta v > 0.5\,\mathrm{km\,s^{-1}}$.

The total cooling rate in the CO lines from HH 54 is found to be $L_{\rm CO} = 1.0\,10^{-2}\,\mathrm{L_\odot}$. The thickness of the emitting layer is $\mathrm{d}r = N(\mathrm{H_2})/n(\mathrm{H_2}) = 2.5\,10^{15}$ cm and, hence, the mass of the molecular material is $6.8\,10^{-3}\,\mathrm{M_\odot}$.

For the lower rotational transitions, the predictions of our model can be compared to observations obtained from the ground. Towards HH 54, spectra of CO (1–0) and (2–1) have been obtained with the 15 m SEST (L. Knee, private communication). At $5.0\,\mathrm{km\,s^{-1}}$ from line centre, the intensities are $T_{\rm mb}(1\text{–}0) = (0.36 \pm 0.06)$ K and $T_{\rm mb}(2\text{–}1) = (0.71 \pm 0.08)$ K. The corresponding values of our model would be somewhat less than 0.075 K and 0.82 K for the (1–0) and (2–1) transitions respectively. It thus appears

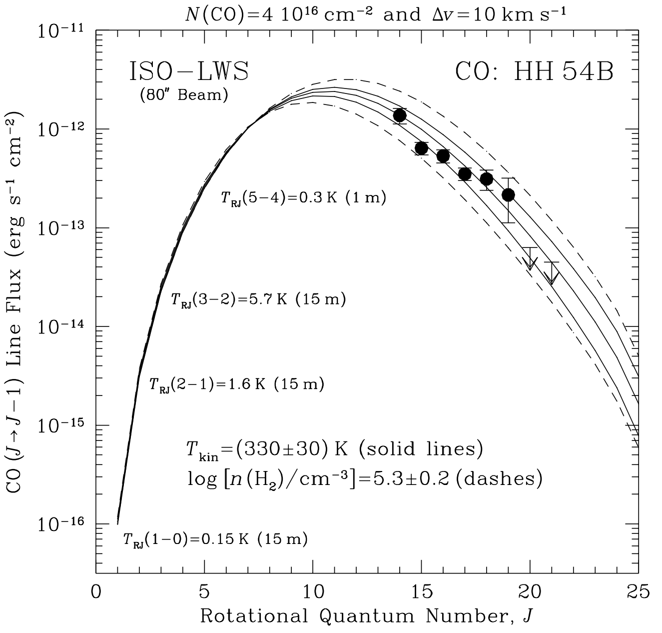

Fig. 2. Observed CO line fluxes towards HH 54 as function of the rotational quantum number of the upper state are compared to model calculations described in the text. Shown errors are statistical and are 1 σ for unblended lines and 2 σ for blends and upper limits. The predicted radiation temperatures of the lower transitions for 15 m and 1 m telscopes are also indicated

that the observed lowest transition is dominated by the cold component (~ 15 K) of the extended outflow, whereas the warm gas contributes significantly to the (2–1) line. This assertion could be further tested by (2–1) mapping and SEST observations in the (3–2) line for which the predicted on-source radiation temperature is 5.7 K.

4.2. The H_2O and OH spectra

Keeping all parameters of the CO model of HH 54 fixed, we computed the ortho- and para-water spectra with the H_2O abundance, $X(H_2O)$, as the only free parameter. For both, the number of included energy levels was 45, involving 164 transitions, several of which are masing. The radiative transition rates are those of Chandra et al. (1984), whereas for the collision rates we used the H_2O–He values ($\times 1.35$) presented by Green et al. (1993). The distribution of the ortho and para forms was assumed to be in the ratio of the statistical weights of their nuclear spins (3 : 1). As for the CO computations, the radiation field included both the cosmic microwave background and that of the diffuse dust emission (Sect. 3), the effects of which on the level populations are relatively minor, though.

The data are well represented by the adopted CO model and a water abundance $X(H_2O) = 10^{-5}$, i.e. $[H_2O/CO] \sim 10^{-1}$. Similarly, this model fits the OH spectrum as well, for $X(OH) = 10^{-6}$ (44 transitions from the HITRAN database, Rothman et al. 1987, with collision rate coefficients from Offer et al. 1994). In Fig. 3, the modeled

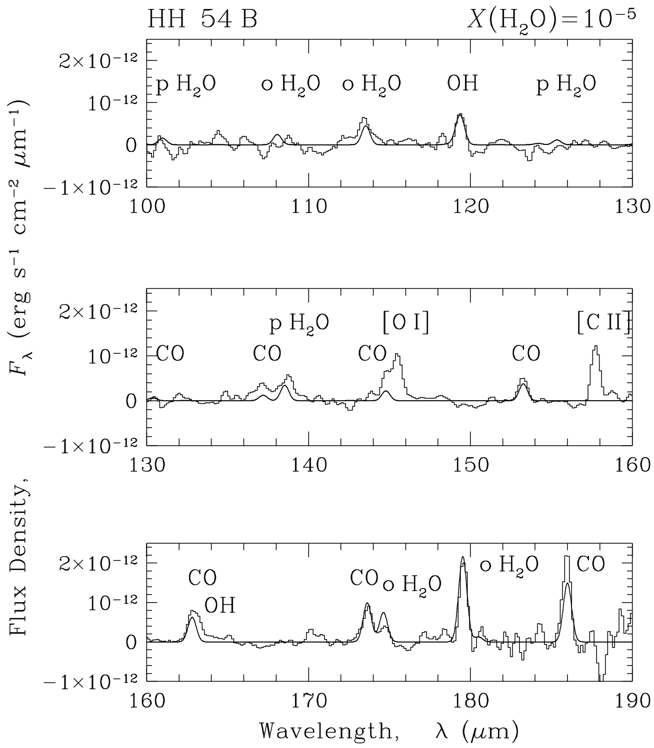

Fig. 3. The computed H_2O, OH and CO spectra, convolved with the LWS instrumental profile for $R(\lambda)$, are shown by the continuous line, superposed onto the LWS observations of HH 54, displayed in histogram form. The abundances for the fit are $X(OH) = 10^{-6}$ and $X(H_2O) = 10^{-5}$

intensities of CO, OH and H_2O, convolved with the instrumental profile, are shown superposed onto the observed spectral line data. The water spectrum is very sensitive to changes of the model parameters: the fact that the 179.5 μm line, connecting to the ground state of ortho-H_2O, is observed to be the strongest, puts severe constraints on both the temperature and density of the emitting gas. The overall success of the model, viz. the capability to simultaneously fit the CO, OH and H_2O observations, lends credence to the probable uniqueness of our model of HH 54.

The H_2O lines identified in Fig. 3 originate from levels within $E/k \sim 300$ K above ground and, with the exception of the 138.5 μm para-line, are all optically thick ($\tau \gtrsim 1$ to ~ 70). The opacity in the 557 GHz ortho ground state transition is $\tau \sim 60$ and we predict a line temperature of about 0.3 K for future observations with the 1 m-dish aboard the Odin satellite. The total rotational line cooling, due to both ortho- and para-H_2O, amounts to $L_{H_2O} = 2.0\,10^{-3}\,L_\odot$, i.e. about 20% of that due to CO, being ten times more abundant. The OH cooling rate is half of that of H_2O. Hence, the radiative losses from HH 54 through CO, OH and H_2O line emission are $\sim 1.3\,10^{-2}\,L_\odot$. Anticipating the results of the next section, the mechanical power input is $L_k = \frac{1}{2}\,\mu\, m_H\, n_0\, v_s^3 \times area = 1.8\,10^{-2}\,L_\odot$, so that more than 70% is radiated away in the CO, OH and H_2O lines. In view of the uncertainties involved it is not excluded that essentially all (with some dust cooling) of the shock luminosity is radiated by these species alone.

4.3. Excitation of the molecules

In the absence of a strong radiation field the most likely physical mechanism of excitation of HH 54 is collisional heating by shock waves. The relatively low temperatures derived above (~ 300 K) are indicative of rather slow shocks, whose velocities are of order $10\,\mathrm{km\,s^{-1}}$. The compression of the gas behind the shocks is given by $n_{max}/n_0 = C\,v_s/p$, where $C = 77$ for v_s in $100\,\mathrm{km\,s^{-1}}$, and where $p = B_{0\perp}/n_0^q$ relates the normal component of the pre-shock magnetic field, $B_{0\perp}$, to the pre-shock density, n_0 (see: Hollenbach et al. 1989). Crutcher et al. (1993) found $B_{0\perp} < 16\,\mu$G for dark clouds (average density $n(\mathrm{H}) \sim 2\,10^3\,\mathrm{cm^{-3}}$) so that $p \lesssim 0.4$ for $q = 0.5$. Taking n_{max} to be the observed post-shock value of the volume density, i.e. $2\,10^5\,\mathrm{cm^{-3}}$, and using $v_s = 10\,\mathrm{km\,s^{-1}}$ leads to $n_0(\mathrm{H_2}) \lesssim 10^4\,\mathrm{cm^{-3}}$. The value of p is uncertain by at least a factor of two, affecting the estimate of the pre-shock density accordingly.

Kaufman & Neufeld (1996) have recently presented detailed model calculations of molecular, non-dissociative C-shocks. The lowest pre-shock density ($10^4\,\mathrm{cm^{-3}}$) considered in these models is of the order of our estimate for the conditions in HH 54. Low-velocity models for $\log n(\mathrm{H_2}) = 4.0$ reproduce our CO, OH and H_2O observations very well, with the observed line *ratios* falling in between the models for $v_s = 10\,\mathrm{km\,s^{-1}}$ and $15\,\mathrm{km\,s^{-1}}$ respectively. On the basis of the previously estimated source solid angle, viz. $\Omega_{source} = 1.8\,10^{-8}$ sr (Sect. 4.1), the lower shock velocity of $10\,\mathrm{km\,s^{-1}}$ would be favoured by the model's *absolute* fluxes. In this case, model fluxes would be in very good agreement with the observations, i.e. within the observational error of the brighter lines, the exception being the OH 119 μm doublet which would appear underestimated by the model by a factor of two to three.

Although the identification of C-shocks as the exciting agent of the molecules seems basically correct in the case of HH 54, a few comments may be in order. (1) The C-shock models have been computed for planar, stationary shock waves. However, our estimates of the shock parameters are close to those where C-shocks may become unstable, developing cooler clumps of neutral material (Wardle 1990). The clumpy morphology of HH 54 would be qualitatively in accord with such a scenario. In addition, the brightness variability of the H_2 (1, 0) S(1) line reported by Gredel (1994) is a clear indicator of non-stationary flows: the time scale of this variability $\lesssim 10$ yr, significantly shorter than the flow time scale, which is estimated to be $\sim 10^2$ yr. (2) The models assume that $p = 1.0$, implying *uncompressed* field strengths of at least 141 μG. This certainly appears excessive for *dark clouds* by large factors. The effect of a significantly reduced value of p would be to *increase* the post-shock temperature (Hollenbach et al. 1989). When comparing with observations, this could mean that one is using the incorrect diagnostics. (3) Emission from higher excitation material, e.g. in the NIR, is outside the domain of C-shock excitation. A unifying shock model would thus be desirable. E.g., models of wide bow shocks have yet to be developed to the level of sophistication as those of Kaufman & Neufeld. Needless to say that further progress on the observational side would require improved spatial and spectral resolution.

5. Conclusions

In short, we conclude the following:

1. The shocked flow HH 54 has been successfully observed with the LWS. The spectrum of thermally excited H_2O lines is the first obtained towards an HH-object.
2. The high-J CO transitions present in the spectrum are used to estimate the physical characteristics of the line emitting regions. This CO model fits simultaneously also the observed OH and H_2O spectra for abundances $X(\mathrm{OH}) = 10^{-6}$ and $X(\mathrm{H_2O}) = 10^{-5}$ respectively.
3. Essentially all of the weak-shock energy of HH 54 is dissipated in rotational lines of CO, OH and H_2O.

Acknowledgements. RL enjoyed interesting discussions with M. Kaufman and D. Neufeld and we thank them for making available to us the results of their C-shock models. We thank P. Bergman for the LVG code and appreciate the valuable suggestions made by the referee, E. van Dishoeck.

References

Chackerian C.Jr., Tipping R.H., 1983, J.Mol.Spec. 99, 431
Chandra S., Varshalovich D.A., Kegel W.H., 1984, A&AS 55, 51
Clegg P.E. et al., 1996, this volume
Crutcher R.M., Troland T.H., Goodman A.A., Heiles C., Kazès I., Myers P.C., 1993, ApJ 407, 175
Graham J.A., Hartigan P., 1988, AJ 95, 1197
Gredel R., 1994, A&A 292, 580
Green S., Maluendes S., McLean A.D., 1993, ApJS 85, 181
Hollenbach D.J., Chernoff D.F., McKee C.F., 1989, in: Proc. 22nd Eslab Symp. on Infrared Spectroscopy in Astronomy, ESA SP-290, p. 245
Kaufman M.J., Neufeld D.A., 1996 ApJ 456, 611
Kessler M. et al., 1996, this volume
Knee L.B.G., 1992, A&A 259, 283
Nisini B. et al., 1996, this volume
Offer A.R., van Hemert M.C., van Dishoeck E.F., 1994, v J. Chem. Phys. 100, 362
Rothman L.S. et al., 1987, Appl. Opt. 26, 4078

Schinke R., Engel V., Buck U., Meyer H., Diercksen G.H.F., 1985, ApJ 299, 939
Schwartz R.D., Dopita M.A., 1980, ApJ 236, 543
Swinyard B.M. et al., 1996, this volume
Wardle M., 1990, MNRAS 246, 98

This article was processed by the author using Springer-Verlag LaTeX A&A style file *L-AA* version 3.